

Coronal hole boundaries evolution at small scales: I. EIT 195 Å and TRACE 171 Å view

M. S. Madjarska^{1,2} and T. Wiegelmann¹

¹ Max-Planck-Institut für Sonnensystemforschung, Max-Planck-Str. 2, 37191 Katlenburg-Lindau, Germany

² Armagh Observatory, College Hill, Armagh BT61 9DG, N. Ireland

Received date, accepted date

ABSTRACT

Aims. We aim at studying the small-scale evolution at the boundaries of an equatorial coronal hole connected with a channel of open magnetic flux with the polar region and an ‘isolated’ one in the extreme-ultraviolet spectral range. We intend to determine the spatial and temporal scale of these changes.

Methods. Imager data from TRACE in the Fe IX/X 171 Å passband and EIT on-board Solar and Heliospheric Observatory in the Fe XII 195 Å passband were analysed.

Results. We found that small-scale loops known as bright points play an essential role in coronal holes boundaries evolution at small scales. Their emergence and disappearance continuously expand or contract coronal holes. The changes appear to be random on a time scale comparable with the lifetime of the loops seen at these temperatures. No signature was found for a major energy release during the evolution of the loops.

Conclusions. Although coronal holes seem to maintain their general shape during a few solar rotations, a closer look at their day-by-day and even hour-by-hour evolution demonstrates a significant dynamics. The small-scale loops (10''–40'' and smaller) which are abundant along coronal hole boundaries have a contribution to the small-scale evolution of coronal holes. Continuous magnetic reconnection of the open magnetic field lines of the coronal hole and the closed field lines of the loops in the quiet Sun is more likely to take place.

Key words. Sun: atmosphere – Sun: corona – Methods: observational – Methods: data analysis

1. Introduction

Coronal holes (CHs) are large regions on the Sun that are magnetically open. They are identified as the source of the fast solar wind ($\sim 800 \text{ km s}^{-1}$) (Krieger et al. 1973) and are visible in coronal lines (formed at temperatures above $6 \cdot 10^5 \text{ K}$) as regions with a reduced emission relative to the quiet Sun (Wilhelm 2000; Stucki et al. 2002). There are two types of coronal holes: polar and mid-latitude CHs. During the minimum of solar activity the solar atmosphere is dominated by two large CHs situated at both polar regions. The mid-latitude CHs can be either ‘isolated’ or connected with a channel of open magnetic flux to a polar CH. The latter are called equatorial extensions of polar CHs (EECHs). The isolated coronal holes have an occurrence rate that follows the solar activity cycle and are usually connected with an active region (Insley et al. 1995).

Huber et al. (1974) compared the appearance and physical parameters of the different layers of the solar atmosphere in and outside coronal holes (e.g. the quiet Sun) using the Apollo Telescope Mount on Skylab. Their measurements of the height of emission of various ions at different ionisation stages (different formation temperatures) at the polar limb indicated an increase of the thickness of the transition region underlying coronal holes. Hence, they found a difference between quiet Sun and coronal holes already pronounced at transition region temperatures.

Feldman et al. (1999) studied the morphology of the upper solar atmosphere using high-resolution data (1''–2'') taken by

Transition Region and Corona Explorer (TRACE) and Solar Ultraviolet Measurements of Emitted Radiation spectrometer (SUMER) on-board SoHO, and the Naval Research Laboratory spectrometer on SKYLAB. The authors found that in the temperature range $4 \cdot 10^4 \text{ K} \leq T_e \leq 1.4 \cdot 10^6 \text{ K}$ the upper solar atmosphere is filled with loops of different sizes with hotter and longer loops overlying the cooler and shorter loops (Dowdy et al. 1986). At heights above $2.5 \cdot 10^4 \text{ km}$ in the upper solar atmosphere of the quiet Sun only loops at temperatures $T_e \sim 1.4 \cdot 10^6 \text{ K}$ exist. No distinction was found between quiet Sun and coronal hole morphology at $5 \cdot 10^4 \leq T_e \leq 2.6 \cdot 10^5 \text{ K}$. That suggests that both regions are filled with structures at similar sizes which are emitting at similar temperatures. These structures do not exceed a height of 7 Mm and have lengths $\leq 21 \text{ Mm}$. Feldman et al. (1999) also investigated the coronal hole boundaries concluding that they are seeded with small-scale loops ($< 7 \text{ Mm}$). There coexist, however, long loops at temperatures above $T \sim 1.4 \cdot 10^6 \text{ K}$ which generally originate from the same location but close at faraway locations.

Wiegelmann & Solanki (2004) made a further step by reconstructing the magnetic field in coronal holes and the quiet Sun with the help of a potential field model. They found that the CHs loops are on average shorter, lower and flatter than in the QS. High and long closed loops are extremely rare in CHs, whereas short and low loops are almost abundant as in the QS region. This result strongly supports the observational findings on the structure of the upper solar atmosphere in the quiet Sun and coronal holes.

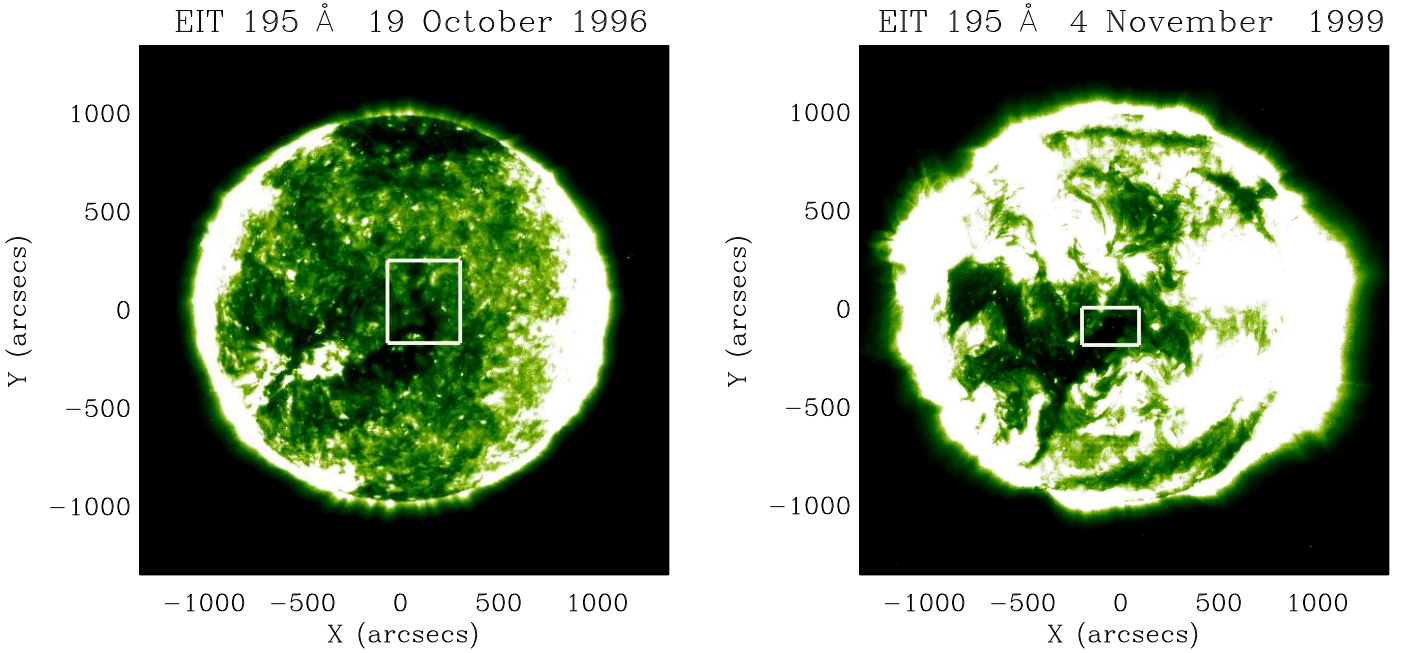


Fig. 1. Full-disk EIT 195 Å images obtained on 1996 October 19 and 1999 November 4. The over-plotted boxes outline the field-of-views subject to a detailed study.

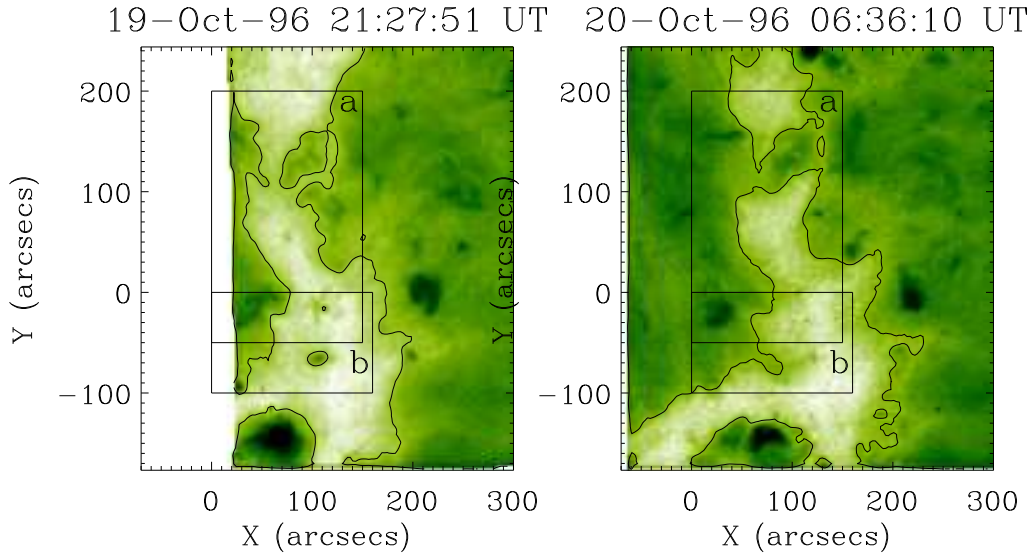


Fig. 2. Color table reversed EIT 195 Å images of the coronal hole observed on October 19-20, 1996. The over-plotted rectangular areas (a and b) are shown enlarged in Figs. 3 and 4.

Based on SKYLAB data in soft X-rays Timothy et al. (1975) first reported the distinctive feature of the EECHs to exhibit quasi-rigid rotation. Shelke & Pande (1985) found that equatorial CHs (without dividing them in different classes) have a rotational period which is a function of latitude and thus exhibit differential rotation. Navarro-Peralta & Sanchez-Ibarra (1994) showed that isolated CHs have a typical differential rotation, while EECHs maintain two types of rotation rates: differential below a latitude of 40° which becomes almost rigid while ap-

proaching the poles. Insley et al. (1995) concluded that mid-latitude CHs rotate more rigidly than the photosphere, but still exhibit significant differential rotation.

Due to the different rotation profiles at coronal and photospheric level and the fact that CH boundaries (CHBs) separate two topologically different (open and closed) magnetic field configurations, CHBs are presumably the regions where processes take place that open and close magnetic field lines. The reconfiguration of the CHBs is believed to happen through magnetic

reconnection between the open and closed magnetic field lines of the CH and the surrounding quiet Sun.

The small-scale evolution of CH boundaries has been a subject of several studies during the last few decades (Kahler & Moses 1990, and the references therein). These studies aimed at understanding the general evolution of coronal holes, the quasi-rigid rotation of EECH compared to the differentially rotating solar photosphere as well as their relation to the slow solar wind generation. Kahler & Moses (1990) studied SKYLAB X-ray images of a single EECH with a time resolution of 90 minutes aimed at looking for discrete changes of the CH boundaries. They found that X-ray bright points (BPs, small-scale loops in the quiet Sun and CHs, for details see Madjarska et al. (2003)) play an important role in both the expansion and contraction of the CH. For this study a single coronal hole observed during the decreasing phase of the solar cycle activity was used. Bromage et al. (2000) reported that small-scale changes of the boundaries of the CH on 1996 August 26 took place on time-scales of a few hours in observations with the EIT in Fe XII 195 Å. The authors, however, do not give any details on the nature of these changes. Kahler & Hudson (2002) made the first systematic morphological study of the boundaries of coronal holes as viewed in soft X-ray images from the Yohkoh Soft X-ray telescope. They studied three coronal holes during several rotations, all formed during the maximum of solar activity cycles 23 and 24. All three coronal holes represent equatorial extensions of polar coronal holes. They found that the CHs evolve slowly, and neither large-scale transient X-ray events nor coronal bright points appeared significant factors in the development of CH boundaries. They suggested that open-close magnetic field reconnection is more likely to describe the actual physics at the CHBs. We should note here that the visibility of BPs in X-ray images is strongly diminished during solar maximum activity by the presence of active regions and bright loops seen in X-rays. The number and size of BPs, and also their lifetime strongly depend on the temperature of which they are observed, with more and longer living BPs seen in spectral lines formed at lower temperatures.

The emergence of magnetic fields in active regions and their subsequent diffusion due to random convective motions in the photosphere influenced by the meridional flow is believed to be the main mechanism leading to the formation of coronal holes. Wang & Sheeley (1994) developed a model where the footpoints exchange between open and closed magnetic field lines (the so called ‘interchange reconnection’) generates coronal holes and maintains their quasi-rigid rotation against the differentially rotating photospheric layers. This type of reconnection process results in an exchange of footpoints between open and closed magnetic field lines with no change in the total amount of open or closed flux (Wang & Sheeley 1994). The reconnection takes place very high in the corona ($r \sim 2.5R_{\odot}$) and occurs continuously in the form of small, stepwise displacements of field lines. According to the authors this scenario may explain why no X-ray signatures have been detected in association with boundary evolution in long-lived coronal holes studied by Kahler & Hudson (2002). They proposed that the blobs emitted from the tops of helmet streamers as radially elongated density enhancements and associated with the slow solar wind are probably the result of this reconnection process.

Our study aims at providing for the first time an analysis on the small-scale (determined by the instrument resolution) evolution of coronal hole boundaries on a time scale from tens of minutes to hours using EUV (EIT/195 Å and TRACE/171 Å) observations with spatial resolution ranging from 1'' (TRACE)

to 5.5'' (EIT). In Section 2 we describe the observational material and data reduction applied. Section 3 presents the data analysis and the obtained results. The discussion and conclusions on the obtained results in the light of the existing theoretical models as well as the future perspectives on the subject discussed in this work are given in Section 4.

2. Observational material and data reduction

We studied two coronal holes, one was observed in October 1996 (hereafter CH1) and the second in November 1999 (hereafter CH2). The CH1 is the well known ‘Elephant trunk coronal hole’, an equatorial extension of north pole CH which has been the subject of several studies (Bromage et al. 2000, and the references therein). CH2 is an ‘isolated’ mid-latitude CH observed in November 1999. Fig. 1 shows EIT images in the 195 Å passband with over-plotted boxes outlining the analysed FOVs for both CHs.

2.1. EIT

The CH1 data were recorded with EIT in the 195 Å passband on 1996 October 19-20 with a full resolution of 2.6''. The images were taken from 20:00 UT (19 October) until 06:00 UT (20 October) every 15 min (except at 05:00 UT). Additionally, we selected full-disk data covering 48 hrs of observations from 15:00 UT on October 18 until 15:41 UT on October 20 taken approximately every 2 hrs. All data related to CH1 were derotated to 07:00 UT on October 20. The data from November 1999 were taken from 15:00 UT on November 3 until 15:00 UT on November 5 and de-rotated to 15:00 UT on November 5. Both datasets have a 5.2'' angular pixel size.

The necessary data reduction was applied, i.e. the images were background subtracted, degripped, flat-fielded, degradation corrected and normalised. They were also derotated to a reference time using the `drot_map.pro` procedure from SolarSoft. The procedure applies synodic values for the differential rotation. Cosmic ray removal was not applied because it was not needed and carries the risk of removing real small-scale structures.

2.2. TRACE

The TRACE data were obtained in Fe IX/X 171 Å on November 4, 1999. The data have a 3 s cadence and a variable exposure time from 00:50 UT to 07:11 UT during approximately 7 hours.

The following corrections were applied: dark current subtraction (obtained the day before), flat-field corrections, spikes and streaks removal. The background diffraction pattern was removed but some residual remained. A normalisation for exposure and a pointing offset correction for the studied channel were also applied.

The data were obtained close to the eclipse period (which started on November 7) during which TRACE is attenuated by the Earth atmosphere in parts of its orbit, and the response in the EUV channels is compromised. However, for several weeks either side of the eclipse period the data are also contaminated. As our data were taken only 3 days before the eclipse started, we had to reduce the number of used images to only 6 (from 434). The images were selected after a careful flux analysis and we are confident that they can be used for the purposes of this study (see later in the text).

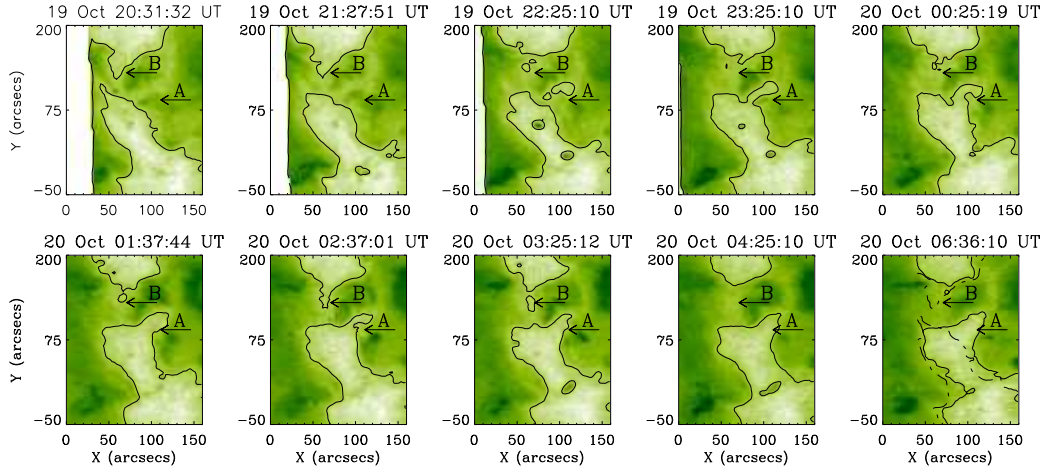


Fig. 3. EIT images of the area marked with ‘a’ in Fig. 2 (reversed color table). The arrows point at the BPs whose evolution led to the expansion (arrow A) and the contraction (arrow B) of the CH. The over-plotted dashed-dotted line shows the boundary from the first image.

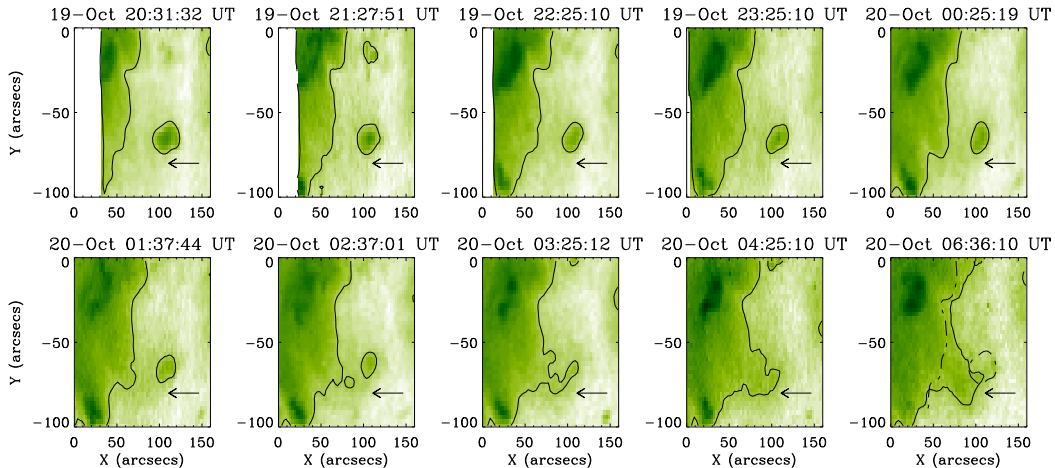


Fig. 4. EIT images of the area marked with ‘b’ in Fig 2 (reversed color table). The arrows point at a bright point whose evolution led to the contraction of the coronal hole. The over-plotted dashed-dotted line shows the boundary from the first image.

In both imagers (EIT and TRACE) the measured values are in data numbers (DN). Data number is the output of the instruments electronics which corresponds to the incident photon signal converted into charge within each CCD pixel. The contours were smoothed in order to remove changes due to image irregularities which could be unreal changes.

3. Data analysis and results

In the present work we paid special attention on the data reduction in order to get reliable information on the evolution of CH boundaries using a contour plot. This method is more reliable than a visual inspection and ensures the detection of any small-

scale changes. The contours have different values for the data with different resolution. The contour values also depend on the observed temperatures with coronal holes expanding at higher temperatures (Bromage et al. 2000). For the present study we determined the boundaries as the region which has intensities 1.5 times the average intensity of the darkest region inside the coronal hole. The visual inspection showed that this value describes well the boundaries as determined using He I 10830 Å images from Kitt Peak National Observatory (Henney & Harvey 2005). For the TRACE 171 Å images of CH2 we used an EIT image obtained in Fe XII 195 Å in order to establish the CHBs. The Fe IX/X 171 Å passband has a transition region emission contribution and is, therefore, not well suited to determine CHBs.

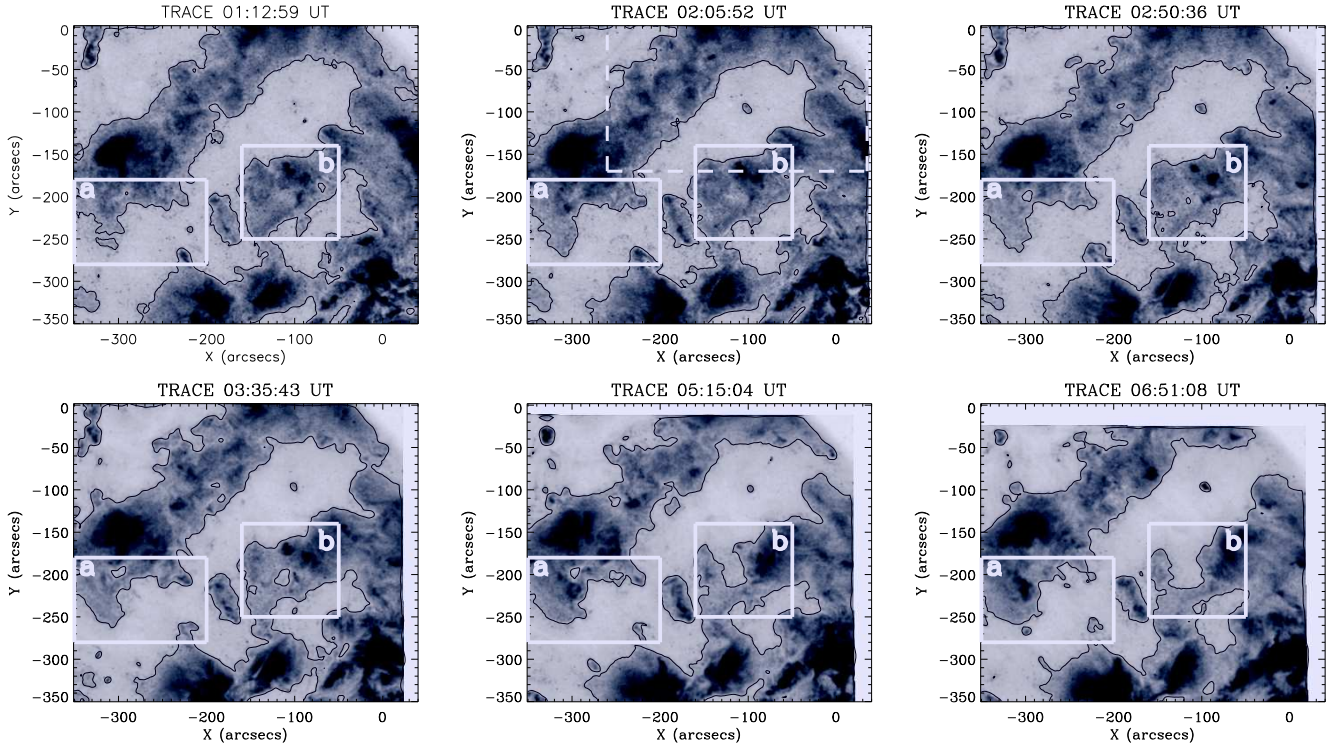


Fig. 5. Reversed color TRACE 171 Å images showing partial field-of-view of CH2 observed in November 1999. The over-plotted rectangular areas (a and b) are shown enlarged in Figs 6 and 7. The dashed line box corresponds to the field-of-view presented in Fig. 8.

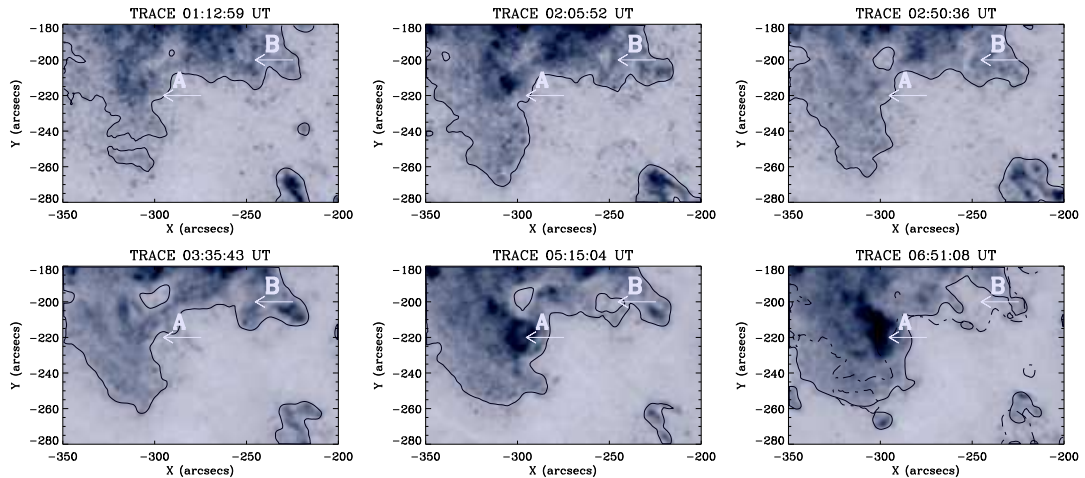


Fig. 6. TRACE 171 Å images marked with ‘a’ in Fig. 5 and showing a contraction of the CH due to the formation of a new BP (arrow A) close to the CH boundary and an expansion due to the disappearance of a BP (arrow B). The over-plotted dashed-dotted line shows the boundary from the first image.

We selected two images (EIT and TRACE) obtained at the same time, applied the necessary offset correction, over-plotted on the TRACE images the boundaries as determined by EIT and then established for TRACE its own contour of constant flux which matches well the EIT contour.

In order to follow the evolution of the CHs for the longest possible period of time we produced movies from full-disk images obtained with EIT in the 195 Å passband. An important issue analysing these images was the projection effect of loops at the CHBs which can mimic changes which are not real. To avoid this problem we have chosen images showing the CHs with the

eastern and western boundaries not further than $-300''$ and $300''$ from the disk center, respectively. The movies can be seen online as movie_1996.mp4 (CH1) and movie_1999.mp4 (CH2). The animated sequences show derotated images of the coronal holes with their boundaries outlined with a solid line. A dashed-dotted line contour corresponds to the first image of the sequence.

Following the CHs boundaries evolution during 48 hrs we see a significant dynamics related to the evolution of the small-scale loops known as BPs. BPs represent $\approx 10''$ – $40''$ features with enhanced intensity. Their appearance is subject of the spatial resolution of the instrument, so they are often

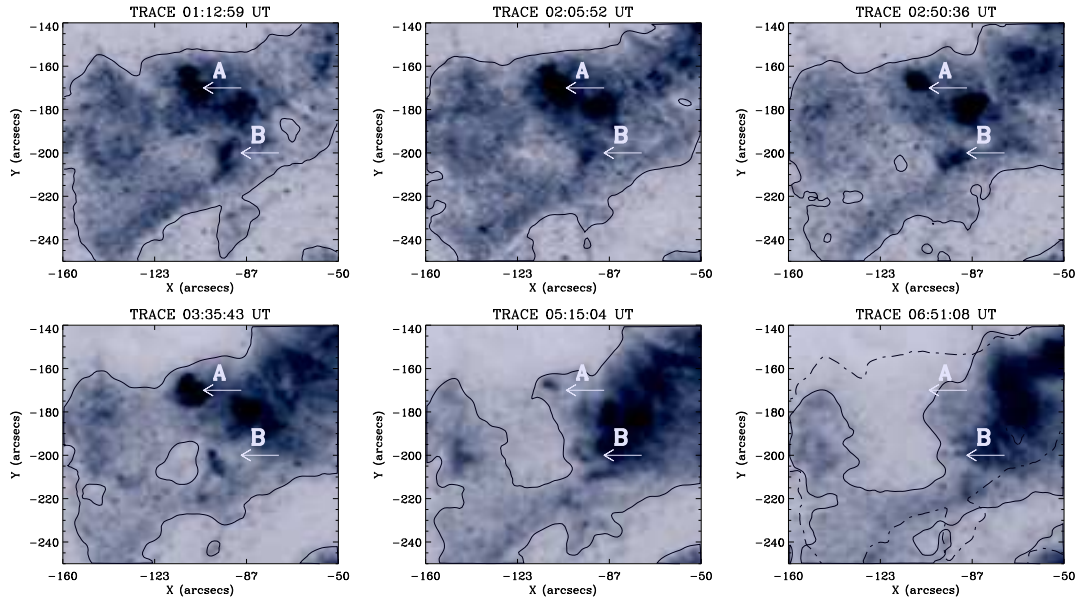


Fig. 7. TRACE 171 Å images marked with 'b' in Fig. 5 showing a large expansion of the coronal hole due to the disappearance of two BPs (arrows A and B). The over-plotted dashed-dotted line shows the boundary from the first image.

seen as a bright core surrounded by a diffuse cloud. High-resolution observations ($1''$ – $2''$) show that BPs consist of several small loops (Sheeley & Golub 1979; Ugarte-Urra et al. 2004; Pérez-Suárez et al. 2008). Only BPs which are close to the CHBs play a role in the expansion or contraction of the CHs. We do not identify any flaring events related to this evolution. For the narrow CH1, the emergence, evolution and disappearance of BPs results in some cases in a complete displacement of parts of the CH in either eastern or western direction (see the CH1 movie). Madjarska et al. (2004) analysed SUMER spectral lines taken along a part of the CH1. The authors found numerous transient features called explosive events located along the CH boundaries as well as around the BP which is inside the CH (Fig. 1). We also observe displacements of the boundaries which are not related to any well distinguishable structure in EIT 195 Å or TRACE 171 Å. A check on temporally close images taken in the EIT He 304 Å ($T \sim 4 \cdot 10^4$ K) channel shows clearly the existence of a BP which apparently has a low temperature and therefore cannot be seen in the hotter passbands. The time scale of the changes is defined by the lifetime of the BPs which is around 20 hrs in EUV at coronal temperatures (Zhang et al. 2001) and 8 hrs in X-rays (Golub et al. 1974).

The next step in our analysis was to study individual cases of evolving loop structures (BPs) and their contribution to the coronal hole evolution in more detail. The analysed FOV for CH1 is shown in Fig. 2 presented by two images taken at two different times. The two overplotted rectangular boxes (a and b) are shown enlarged in Figs. 3 and 4. The two arrows (A and B) on Fig. 3 are pointing at loop structures (i.e. BPs) whose evolution led to a change of the boundary. In Fig. 3 the arrow A shows the disappearance of a BP associated with an expansion of the coronal hole while the arrow B is pointing at the appearance of a loop structure which led to a contraction of the CH. These changes correspond to the size of the evolving BPs. In Fig. 4 another BP evolution is followed by a contraction of the CH.

The CH2 is presented in Fig. 5 by images taken at almost regular time intervals (e.g 01:12, 02:00, 02:50, 03:38, 05:15 and 06:49 UT). The two over-plotted boxes (a and b) have an en-

larged FOV shown in Figs. 6 and 7. In Fig. 6 one can see that a formation of a new BP (arrow A) led to the contraction of the CH while the disappearance (arrow B) again expanded the CH. In Fig. 7 the disappearance of two BPs is followed by a large increase of the CH region.

4. Discussion and conclusions

The major objective of our study was to determine the dynamics of coronal hole boundaries as seen in the EUV spectral range. To our knowledge similar studies have only been made in the X-ray spectral domain (Kahler & Moses 1990; Kahler & Hudson 2002) which is sensitive to plasmas emitting at temperatures above 3 MK. The examples selected for this study represent an equatorial extension of a polar coronal hole which existed for 4 solar rotations (during the studied rotation the connection was closed above 40°) and an 'isolated' coronal hole. Although the coronal holes seem to maintain their general shape during a few solar rotations, a closer look at their day-by-day and even hour-by-hour evolution demonstrates a significant dynamics. We found that small-scale loops ($30''$ – $40''$) which are abundant along coronal hole boundaries at temperatures up to $T \sim 1.2$ – 1.4×10^6 K have a major contribution to the evolution of coronal holes. The loops (BPs) emergence, evolution and disappearance lead to a continuous expansion or contraction of the coronal holes. In some cases that can result in closing a narrow coronal hole or a large shift of the entire CH. These changes appear to be random probably defined by photospheric processes such as convective motions, meridional flow, differential rotation, emergence of magnetic flux as well as intensive inflow of unipolar magnetic flux from attached active region(s). That most probably triggers intensive magnetic reconnection of the closed magnetic field lines of the quiet Sun and the open ones of the coronal hole. The spectroscopic study of CH1 by Madjarska et al. (2004) found evidence for magnetic reconnection processes happening at transition region temperatures along the CH1 boundaries which strongly supports the results of the present work.

How does the appearance and disappearance of BPs transform the boundaries of the coronal holes? We know so far that

88% of X-ray BPs are associated with converging magnetic polarities (Webb et al. 1993) and most of the BPs are related to cancelling magnetic features. Usually one of the magnetic polarities involved is stronger than the other one (Madjarska et al. 2003) and after the full cancellation of the weaker polarity the remnant one either joins the CH dominant polarity (if it is of the same sign), expanding the CH surface, or forms a new connection (closed magnetic field lines) which triggers contraction of the CH boundaries. This scenario will be tested by applying magnetic field extrapolation on Michelson Doppler Imager data in high-resolution mode for CH2 as well as new forthcoming data from SOT/Hinode. An example with potential field extrapolations from SOHO/MDI is shown in Fig. 8. In future we are planning to study the connection between the magnetic and thermal boundary of coronal holes in more detail with the help of extrapolations from full disk magnetograms from SDO/HMI, which will provide the global topology of the coronal magnetic field and allow to distinguish clearly between globally open and closed regions. The temporal evolution of the fine structure at the coronal hole boundary can be studied with higher resolution and good signal to noise vector magnetograms from Hinode/SOT. In principal it would be also useful to use more sophisticated magnetic field models as the potential field used here. It is well known that the nonlinear force-free approach is superior for modelling of active regions, but unfortunately this approach might not be totally appropriate for coronal hole and quiet sun regions, due to the finite beta plasma in the quiet sun (Schrijver & van Ballegoijen 2005). Consequently one should model the magnetic field and plasma self-consistently, in lowest order with a magneto-hydro-static model as described in Wiegmann & Neukirch (2006). Such an approach is also assumed to automatically provide consistency between thermal and magnetic boundaries of coronal holes. We believe that possible differences between thermal (as identified in EUV images) and magnetic hole boundaries might be an artefact of using to simple magnetic field models.

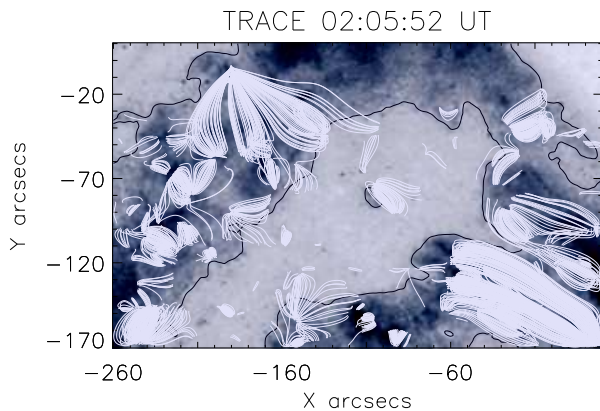


Fig. 8. TRACE 171 Å images with a field-of-view as shown in Fig. 5 with over-plotted only closed magnetic field lines connecting magnetic polarities above 20 G. The magnetic field lines were obtained with a potential magnetic field extrapolation (Wiegmann et al. 2005).

How do our results contribute to the understanding of the mechanism maintaining the rigid rotation of equatorial extension of coronal holes? The rotation of coronal holes is usually determined by measuring their centers during several rotation

e.g. determine their Carrington longitude from rotation to rotation (Navarro-Perralta & Sanchez-Ibarra 1994). These measurements, however, do not take into account the small-scale evolution of coronal holes. Our analysis shows that especially in the case of narrow coronal holes the open magnetic flux could be totally ‘recycled’ (Close et al. 2004, 2005) by the continuous interaction with the closed magnetic flux and therefore in the following rotation the appearance of the coronal hole will be the result of complex changes. An example is the CH1 which almost completely disappeared in September 1996 and reappeared again in August 1996.

New studies based on specially designed and already carried out observing programs with SUMER/SoHO, EIS, XRT and SOT/Hinode and TRACE during the last two years are ongoing which will present the XRT/Hinode view (paper II) and EIS and SUMER view (paper III). These works should reveal more on the physical nature of the reported changes as well as a possible relation between the activity along the coronal hole boundaries and the origin of the slow solar wind.

Acknowledgements. MM thanks ISSI, Bern for the support of the team “Small-scale transient phenomena and their contribution to coronal heating”. Research at Armagh Observatory is grant-aided by the N. Ireland Department of Culture, Arts and Leisure. We also thank STFC for support via grants ST/F001843/1 and PP/E002242/1. The work of TW was supported by DRL-grant 50 OC 0501. SoHO is a mission of international collaboration between ESA and NASA.

References

- Bromage, B. J. J., Alexander, D., Breen, A., et al. 2000, *Sol. Phys.*, 193, 181
- Close, R. M., Parnell, C. E., Longcope, D. W., & Priest, E. R. 2004, *ApJ*, 612, L81
- Close, R. M., Parnell, C. E., Longcope, D. W., & Priest, E. R. 2005, *Sol. Phys.*, 231, 45
- Dowdy, Jr., J. F., Rabin, D., & Moore, R. L. 1986, *Sol. Phys.*, 105, 35
- Feldman, U., Widing, K. G., & Warren, H. P. 1999, *ApJ*, 522, 1133
- Golub, L., Krieger, A. S., Silk, J. K., Timothy, A. F., & Vaiana, G. S. 1974, *ApJ*, 189, L93+
- Henney, C. J. & Harvey, J. W. 2005, in *Astronomical Society of the Pacific Conference Series*, Vol. 346, *Large-scale Structures and their Role in Solar Activity*, ed. K. Sankarasubramanian, M. Penn, & A. Pevtsov, 261–+
- Huber, M. C. E., Foukal, P. V., Noyes, R. W., et al. 1974, *ApJ*, 194, L115
- Insley, J. E., Moore, V., & Harrison, R. A. 1995, *Sol. Phys.*, 160, 1
- Kahler, S. W. & Hudson, H. S. 2002, *ApJ*, 574, 467
- Kahler, S. W. & Moses, D. 1990, *ApJ*, 362, 728
- Krieger, A. S., Timothy, A. F., & Roelof, E. C. 1973, *Sol. Phys.*, 29, 505
- Madjarska, M. S., Doyle, J. G., Teriaca, L., & Banerjee, D. 2003, *A&A*, 398, 775
- Madjarska, M. S., Doyle, J. G., & van Driel-Gesztelyi, L. 2004, *ApJ*, 603, L57
- Navarro-Peralta, P. & Sanchez-Ibarra, A. 1994, *Sol. Phys.*, 153, 169
- Pérez-Suárez, D., Maclean, R. C., Doyle, J. G., & Madjarska, M. S. 2008, *A&A*, 492, 575
- Schrijver, C. J. & van Ballegoijen, A. A. 2005, *ApJ*, 630, 552
- Sheeley, Jr., N. R. & Golub, L. 1979, *Sol. Phys.*, 63, 119
- Shelke, R. N. & Pande, M. C. 1985, *Sol. Phys.*, 95, 193
- Stucki, K., Solanki, S. K., Pike, C. D., et al. 2002, *A&A*, 381, 653
- Timothy, A. F., Krieger, A. S., & Vaiana, G. S. 1975, *Sol. Phys.*, 42, 135
- Ugarte-Urra, I., Doyle, J. G., Madjarska, M. S., & O’Shea, E. 2004, *A&A*, 418, 313
- Wang, Y.-M. & Sheeley, Jr., N. R. 1994, *ApJ*, 430, 399
- Webb, D. F., Martin, S. F., Moses, D., & Harvey, J. W. 1993, *Sol. Phys.*, 144, 15
- Wiegmann, T. & Neukirch, T. 2006, *A&A*, 457, 1053
- Wiegmann, T. & Solanki, S. K. 2004, *Sol. Phys.*, 225, 227
- Wiegmann, T., Xia, L. D., & Marsch, E. 2005, *A&A*, 432, L1
- Wilhelm, K. 2000, *A&A*, 360, 351
- Zhang, J., Kundu, M. R., & White, S. M. 2001, *Sol. Phys.*, 198, 347